Simulation on soot deposition in in-wall and on-wall catalyzed diesel particulate filters

Hyeonoh Kong, Kazuhiro Yamamoto

Department of Mechanical Systems Engineering, Nagoya University
Furo-cho, Chikusa-ku, Nagoya, Aichi 464-8603, JAPAN
kazuhiro@mech.nagoya-u.ac.jp

Keywords: Catalyst; DPF; Numerical simulation; Diesel exhaust; Computed Tomography

ABSTRACT

In order to decrease the regeneration temperature of diesel soot deposited in the diesel particulate filter (DPF), the catalyzed DPF is generally used. Since the catalyst is made of expensive noble metals such as platinum, it is better to reduce the amount of catalyst. For that purpose, we need to know the influence of the catalyst on the soot deposition process. In this study, the flow and the soot deposition of the catalyzed DPF (CDPF) have been simulated. The substrate structure of the filter was obtained by an X-ray CT technique. Here, two types of the catalyst coating were considered, which were in-wall and on-wall CDPFs. For both cases, we set the same amount of catalyst. The effects of the catalyst on the pressure drop were evaluated by comparing the simulation without the catalyst. The permeability of the catalyst layer was estimated based on the experimental pressure drop. In particular, the contact ratio of the deposited soot and the catalyst layer was discussed to obtain the information on the regeneration efficiency. It was found that, due to the catalyst, the soot deposition process was affected. Resultantly, the pressure drop of the on-wall CDPF was smaller than that of the in-wall CDPF. In the case of the on-wall CDPF, more deposited soot can be contacted with the catalyst layer, suggesting the higher efficiency for the filter regeneration.

1. Introduction

Last year, the 2017 United Nations Climate Change Conference (COP23) was held in Germany, emphasizing the urgent need to accelerate climate action in order to keep global temperatures [1]. From now on, it is necessary to reduce emissions of CO_2, which is the main cause of global warming. In the past decades, because of the high fuel efficiency associated with reduced emission of CO_2, diesel vehicles have an unprecedented growth of their share in the market [2, 3]. However, compared with gasoline vehicles, more soot smaller than 1 μm in diameter is emitted in the exhaust gas, which could penetrate deep into the lungs and might be able to enter the bloodstream and even reach the brain [4, 5]. In order to solve this problem, a diesel vehicle is usually equipped with a ceramic filter called diesel particulate filter (DPF). By using the DPF, fine particles including soot are trapped [2, 6]. However, the latest European emissions legislations (i.e. Euro 6) are set on the basis of both mass and number counts to ensure the control of the ultra-fine particles [7, 8]. Therefore, we need to improve the performance of the DPF continuingly.

Although the various types of filters are employed, the most effective is the wall-flow filter with a honeycomb monolith made of ceramic materials such as cordierite and SiC [8], where the exhaust gas is forced to flow through porous walls for particle filtration [9]. However, as more diesel soot is deposited inside the filter, the filter backpressure increases to decrease the fuel economy and cause possible engine failure [7, 8]. To prevent these problems, the DPF must be periodically regenerated by oxidizing trapped diesel soot [7, 8, 10]. In this process, the relatively high temperature (about 600℃) is required. In order to decrease the regeneration temperature of diesel soot deposited in DPF, the catalyzed DPF (CDPF) is generally used [11, 12]. In previous studies, Sarli et

al. have carried out a regeneration experiment by changing the contact ratio of the soot and the catalyst layer, showing that the soot can be burned at low temperature as the contact ratio is higher [12]. It has been reported that the shape of the catalyst is an important factor for increasing this contact ratio, proposing the needle shape, the fiber shape, the flakes and the star shape for better regeneration efficiency [13, 14]. Although these experimental studies have given useful information, it is difficult to observe the deposition and regeneration processes inside the DPF [15, 16].

Needless to say, since the catalyst is made of expensive noble metals such as platinum, it is better to reduce the amount of catalyst. For that purpose, we need to know the influence of the catalyst on the soot deposition process. Our research group has been simulating the phenomenon in DPF numerically by a lattice Boltzmann method (LBM), which is effective for flow simulation in the porous media flow. So far, we have discussed the flow and the soot deposition in the DPF [17-19].

In this study, the flow and the soot deposition of the catalyzed DPF were numerically simulated. The substrate structure of the filter was obtained by an X-ray CT technique. Here, two types of the catalyst coating were considered, which were in-wall and on-wall CDPFs. For both cases, we set the same amount of catalyst. The effects of the catalyst on the pressure drop were evaluated by comparing the simulation without the catalyst. The permeability of the catalyst layer was estimated based on the experimental results. In particular, the contact ratio of the deposited soot and the catalyst layer was discussed to obtain the information on the efficiency for the filter regeneration.

2. Numerical analysis

In the present numerical simulation, the same approach in our previous study was

used [17-19]. The substrate structure of DPF was measured by an X-ray CT technique. The spatial resolution was 2 μm/pix, corresponding to the grid size in the simulation. Numerical domain with the coordinate system is shown in Fig. 1. Its total size was 560 μm (281 lattices) in the X direction perpendicular to the filter wall, and 120 μm (61 lattices) in the Y direction and 120 μm (61 lattices) in the Z direction. The thickness of the filter wall was 300 μm.

Here, the boundary condition is explained. At the inlet, the inflow velocity was 5.13 cm/s, which was the typical value of driving. The temperature at the inlet was 240 ºC, and the mass fraction of the soot was 0.005 in the exhaust gas. The soot size was 100 nm, corresponding to the typical value of the diesel soot [16]. At four sidewalls (top, bottom, right, and left) in Fig. 1, the slip boundary was applied as a symmetrical boundary. The outlet was set as a free outflow boundary with a constant pressure (atmospheric pressure). A non-slip boundary with zero velocity was adopted on the surface of the filter substrate.

3. Results and discussion

3.1. Estimation of permeability of catalyst layer

First, the permeability of the catalyst layer was estimated based on the experimental data. Figure 2 shows the initial pressure drop of bare DPF, on-wall CDPF, and in-wall CDPF obtained by experiments. It should be noted that the same amount of catalyst was coated in both CDPFs. The inlet velocity which corresponds to the velocity passing through the filter wall was changed widely. According to Fig. 2, the initial pressure drop increased as the flow velocity was raised. Also, it was found that the pressure drops of

CDPFs were larger than that of bare DPF, and that there was no pressure difference between two CDPFs.

In the case of the on-wall CDPF, the thickness of the catalyst layer was the constant of 55 μm. Then, it was easy to estimate the permeability of the catalyst layer based on the Darcy's law in Eq. (1):

$$\Delta P = \frac{\mu \times u}{k} \times \Delta L \qquad (1)$$

where μ is the viscosity, u is the inlet velocity, ΔL is the thickness of the catalyst layer, and k is the permeability. In the simulation, the inlet velocity was 5.13 cm/s. Then, the pressure drop (ΔP) of the difference between the on-wall CDPF and the bare DPF was 511 Pa in Fig. 2. By considering that the viscosity was 2.72×10^{-5} kg/(m · s) and ΔL was 55 μm, the permeability of catalyst layer was found to be 1.5×10^{-13} m^2.

On the other hand, different from the on-wall CDPF, it was difficult to evaluate the thickness of the catalyst layer of the in-wall CDPF, because the catalyst was dispersed deeply inside the filter wall. Therefore, for identifying the catalyst region, we used X-ray CT data of the three-dimensional in-wall CDPF. First, by comparing X-ray CT data of the bare DPF, we distinguished the catalyst region and the filter substrate based on the luminosity contrast of the raw X-ray CT image. Next, the numerical simulation of the exhaust gas flow was conducted by assuming the permeability of the catalyst layer temporarily. In this simulation, the soot deposition was not considered to obtain the initial pressure drops of the bare DPF and in-wall CDPF.

Figure 3 shows numerical results to see the difference between the initial pressure drops of bare and catalyzed filters when the permeability of the catalyst layer was

changed. By matching the experimental data with the numerical pressure drop, it was possible to determine the permeability of the catalyst layer. As found in Fig. 2, the difference of the pressure drops of two filters was 458 Pa. Resultantly, the permeability of the catalyst layer of the in-wall CDPF was 1.9×10^{-13} m^2.

3.2. Effect of catalyst on flow field

Next, the effect of catalyst on the flow field was discussed. Figure 4 shows the 2D image of the flow field in X-Y plane. Three cases of bare DPF, on-wall and in-wall CDPFs were compared. These were obtained at Z = 24 μm. The legend shows the absolute value of three-component velocities, which means that the larger this value is, more quickly the flow passes through the filter substrate. The filter wall is located at 190 μm < X < 490 μm. As seen in Fig. 4(a), the flow direction was largely changed when the exhaust gas entered the filter wall. By comparing three profiles, the effects of the catalyst layer were revealed. In case of the on-wall CDPF, the velocity profile of the flow in the catalyst layer at 135 μm < X < 190 μm was quite similar to that of the bare DPF. In case of the in-wall CDPF, the flow was more accelerated due to the narrower space of the catalyzed filter. Indeed, the maximum velocity of the flow was larger than those of the bare DPF and the on-wall CDPF. However, at the region of more downstream at 300 μm < X, there was no big difference between flow fields of three filters. Therefore, it is derived that the influence of the catalyst layer is more apparent at the upstream of the filter wall.

For further discussion, the pressure distributions were investigated. Figure 5 shows the pressure distributions along the flow direction of the X-axis. The pressure was the averaged value in Y-Z plane. To discuss the initial pressure drop, the pressure was

subtracted by the atmospheric pressure at the filter exit. Three cases of bare DPF, on-wall and in–wall CDPFs were compared. It should be noted that, for both CDPFs, the pressure was increased at the region where the filter was catalyzed. Thus, independent of the on-wall or in-wall CDPF, the pressure drop was enlarged by the effect of catalyst on the flow.

3.3. Soot deposition process

In this section, we discussed the soot deposition process in two catalyzed filters. First, we investigated the influence of the catalyst layer on the soot deposition in the filter. Figure 6 shows the profiles of soot deposition region at different times. Here, t is the elapsed time after we started the simulation of the soot deposition. Four profiles are of the bare DPF, showing slice images in X-Y plane obtained at Z = 56 μm. The original substrate of the filter before the soot deposition is shown in Fig. 6(a). At the early stage of the filtration, the depth filtration occurred, where the soot was deposited inside the filter wall. This process was observed at $t < 4$ s. After that, as seen in Fig. 6(b), all surface pores located at $200\mu m < X < 226$ μm were covered with soot. Subsequently, the surface filtration in Fig. 6(c) was observed, where all soot was trapped by the soot cake layer [15]. As seen in Fig. 6(d) at t = 27 s, the thickness of the soot region was simply increased.

Figures 7 and 8 show the profiles of soot deposition region in X-Y plane obtained at Z = 56 μm. These are the results of in-wall and on-wall CDPFs. The profiles of same periods in Fig. 6 are shown. Compared to Fig. 6(a), some pores in the in-wall CDPF in Fig. 7(a) are smaller due to the catalyst coating. It should be noted that the maximum flow velocities of bare DPF, on-wall and in-wall CDPFs were 38.0, 38.2 and 42.1 cm/s,

respectively. Then, compared to the bare DPF, the flow of the CDPF was found to be accelerated. At the same time, in Figs. 7(b) to 7(d), a part of soot was trapped at different X-Y plane, showing less soot amount deposited in the filter than that in Figs. 6(b) to 6(d). On the other hand, in case of the on-wall CDPF in Fig. 8(a), there is the catalyst layer on the filter wall surface. Then, it was found that, as seen in Figs. 8(b) to 8(d), the filtration occurred on the catalyst layer. That is, only the surface filtration was observed.

For further study, the time-variations of the soot deposition amount (ρ_s) and the pressure drop were examined. The value of ρ_s was the mass of deposited soot divided by the filter volume. Results of bare DPF, on-wall and in-wall CDPFs are plotted in Fig. 9. As seen in Fig. 9(a), the soot deposition amount was increased almost linearly, but the value of the on-wall CDPF was larger. This is because all soot was trapped by the surface filtration due to the catalyst layer. From the time-variation of the pressure drop in Fig. 9(b), it is seen that the pressure drop of the bare DPF and in-wall CDPF increased steeply during the depth filtration [15]. After that, the pressure increase was reduced during the surface filtration. It is recognized that the pressure drop of the on-wall CDPF increased more slowly, because only the surface filtration occurred. Resultantly, after t = 8 s, the pressure drop of the on-wall CDPF was smaller than that of the in-wall CDPF. Needless to say, in the case of the bare DPF, the pressure drop was found to be smallest.

3.4. Contact ratio of deposited soot and catalyst layer

For discussing the filter regeneration, it is important to consider the contact ratio of deposited soot and catalyst layer [12]. Then, the time-dependent of this ratio was

evaluated by Eq. (2).

$$\text{Contact ratio of soot and catalyst (CR)} = \frac{\alpha}{\beta} \quad (2)$$

where α is the lattice number of soot in contact with the catalyst, and β is the lattice number of the catalyst layer distributed in the calculation domain. Figure 10 shows the time-variation of the contact ratio of in-wall and on-wall CDPFs. It is seen that, each contact ratio increased with time, and then showed a constant value. The saturated value of the in-wall CDPF was about 13%, and that of the on-wall CDPF was about 17%. Resultantly, the contact ratio of the on-wall CDPF was higher than that of the in-wall CDPF. Although more studies will be needed, more deposited soot can be contacted with the catalyst layer in the on-wall CDPF, suggesting the higher efficiency for the filter regeneration.

4. Conclusion

In this study, the effects of the catalyst on the flow and the soot deposition were numerically investigated. We considered two types of on-wall and in-wall catalyzed filters (CDPFs). The substrate structure of the filter was obtained by an X-ray CT technique. The following results were obtained.

1. In the case of the on-wall CDPF, the permeability of catalyst layer was simply evaluated based on the Darcy's law. It was 1.5×10^{-13} m^2. On the other hand, for the in-wall CDPF, the permeability of catalyst layer was estimated by matching the experimental data with the numerical pressure drop. Resultantly, the permeability was determined to be 1.9×10^{-13} m^2.

2. By comparing the flow of CDPF with that of bare DPF, the effects of the catalyst layer were revealed. In case of the on-wall CDPF, the velocity profile of the flow in the catalyst layer was quite similar to that of the bare DPF. In case of the in-wall CDPF, the flow was more accelerated due to the narrower space of the catalyzed filter. Indeed, the maximum velocity of the flow was larger than those of the bare DPF and the on-wall CDPF. Through the change of the flow field, the pressure was enlarged at the region where the filter was catalyzed.
3. In case of the on-wall CDPF, only the surface filtration occurred, because the catalyst layer on the filter wall surface trapped the soot. Compared to the in-wall CDPF, the soot deposition amount was larger, showing the smaller pressure drop. On the hand, in case of the in-wall CDPF, the shift from the depth filtration to the surface filtration was observed, and the pressure drop was much larger than that of the bare DPF, because the pores in the filter wall was smaller.
4. For on-wall and in-wall CDPFs, each contact ratio increased with time, and then showed a constant value. The saturated value of the in-wall CDPF was about 13%, and that of the on-wall CDPF was about 17%. Resultantly, the contact ratio of the on-wall CDPF was higher than that of the in-wall CDPF, suggesting the higher efficiency for the filter regeneration.

References

[1] UN Climate Change Conference - November 2017.

[2] X. Wu, F. Lin, H. Xu, D. Weng, Appl. Catal. B 96 (2010) 101-109.

[3] S. Wagloehner, M. Nitzer-Noski, S. Kureti, Chemical Engineering Journal 259 (2015) 492-504.

[4] A. Sydbom, A. Blomberg, S. Parnia, N. stenfors, T. sandstrom, S-E. Dahlen, Eur Respir J 17 (2001) 733-746.

[5] R. Prasad, V. R. Bella, Bulletin of Chemical Reaction Engineering & Catalysis 5 (2) (2010) 69-86.

[6] T. Theodoros, N, Leonidas, S. Zissis, Atmospheric Environment 44 (2010) 909-916.

[7] B. Guan, R. Zhan, H, Lin, Z. Huang, J. Enviornmental Management 154 (2015) 225-258.

[8] V. Palma, P. Ciambelli, E. Meloni, A. Sin, Fuel 140 (2015) 50-61.

[9] M. Schejbla, M. Marek, M. Kubíček, P. kočí, Chemical Engineering Journal 154 (2009) 219-230.

[10] C. Beatrice, S. D. Iorio, C. Guido, P. Napolitano, Experimental Theraml and Fluid Science 39 (2012) 45-53.

[11] U. Junko, O. Akira, W. Shudon, N. Tetsuya, O. Akihiko, Appl. Catal. B 43 (2003) 117-129.

[12] V. D. Sarli, G. Landi, L. Lisi, A. Saliva, A. D. Benedetto, Appl. Catal. B 197 (2016) 116-124.

[13] S. Bensaid, N. Russo, D. Fino, Catalysis Today 216 (2013) 57-63.

[14] P. Miceli, S.Bensaid, N. Russo, D. Fino, Chemical Engineering Journal 278 (2015) 190-198.

[15] E. Wirojsakunchai, E. Schroeder, C. Kolodziej, D.E. Foster, T. Schmidt, N. Root, T. Kawai, T. Suga, T. Nevius, T. Kusaka, SAE paper 2007-01-0320 (2007).

[16] A. G. Konstandopoulos, E. Skaperdas, SAE paper 2002-01-1015 (2002).

[17] K. Yamamoto, M. Nakamura, H. Yane, H. Yamashita, Catalysis Today 153 (2010) 118-124.

[18] K. Yamamoto, K. Yamauchi, Proc. Combustion Institute 34 (2013) 3083-3090.

[19] K. Yamamoto, T. Sakai, Catalysis Today 242 (2015) 357-362.

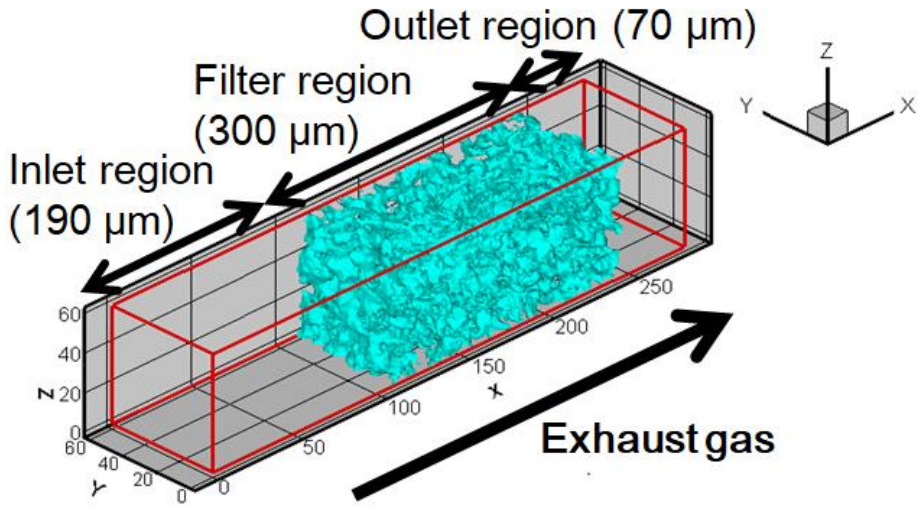

Fig. 1 Numerical domain with coordinate system.

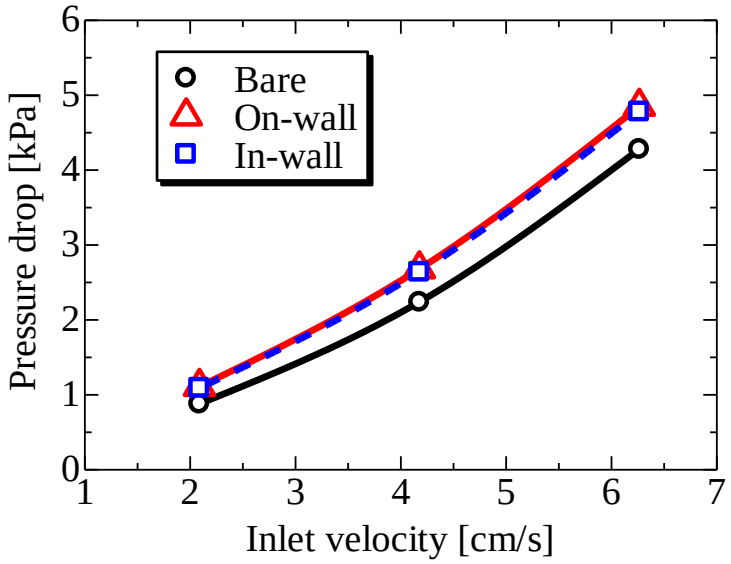

Fig. 2. Initial pressure drop of bare DPF, on-wall CDPF, and in-wall CDPF obtained by experiments.

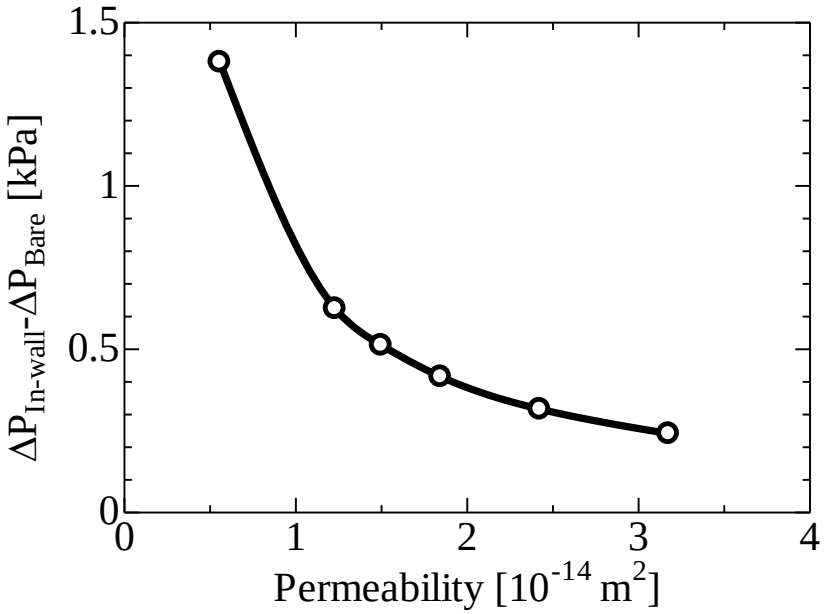

Fig. 3. Numerical results are shown to see difference between the initial pressure drops of bare DPF and in-wall CDPF when the permeability of the catalyst layer was changed.

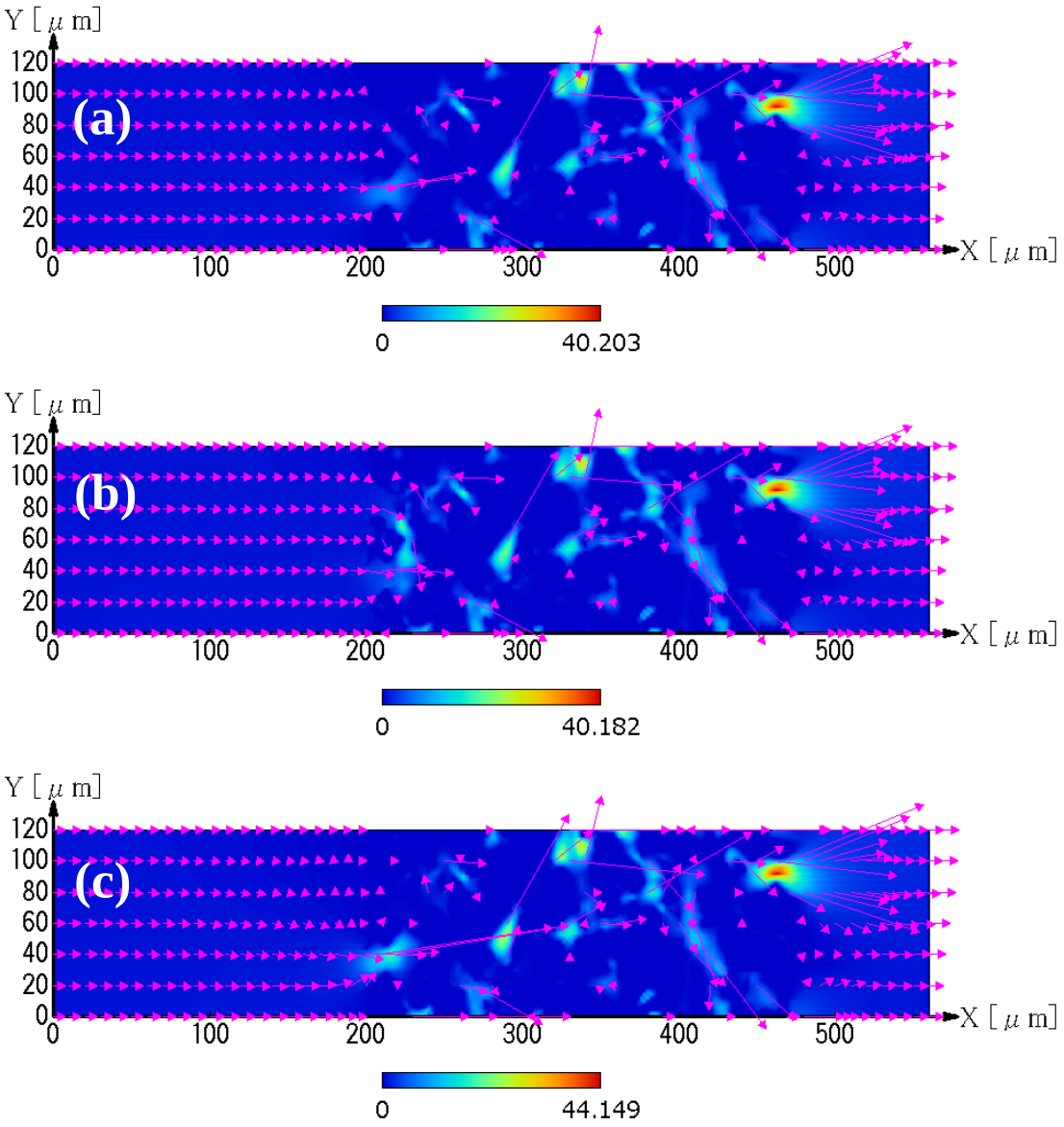

Fig. 4. Flow fields of (a) bare DPF, (b) on-wall CDPF, (c) in-wall CDPF.

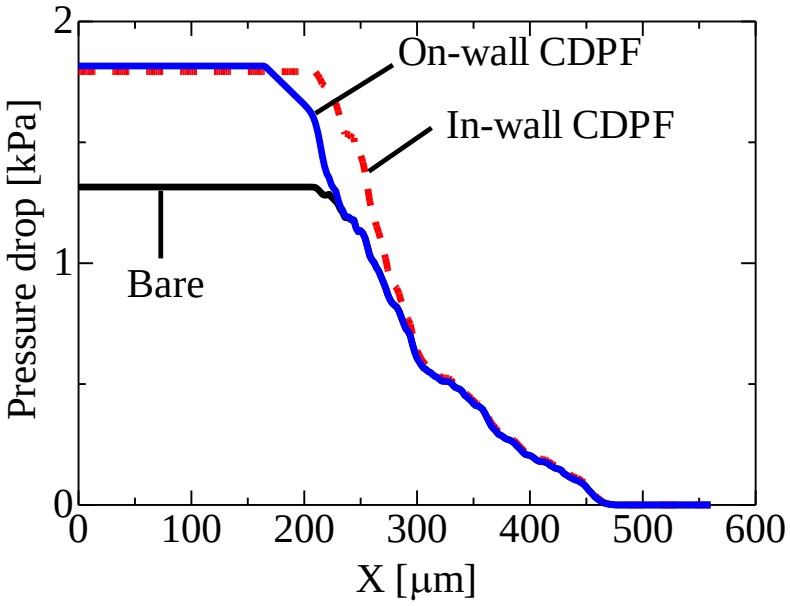

Fig. 5. Pressure distribution along the X direction

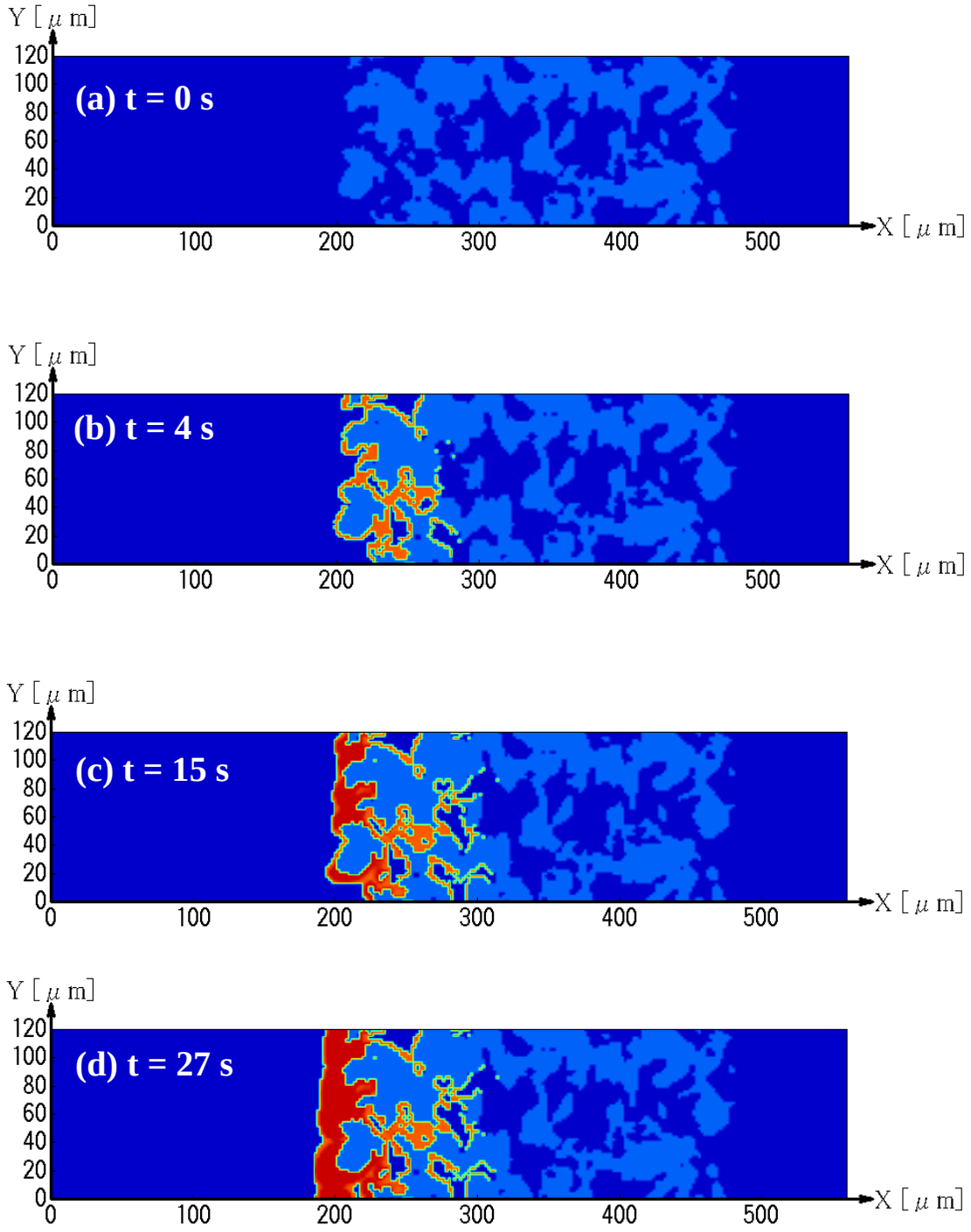

Fig. 6. Profiles of soot deposition region at different times obtained of bare DPF.

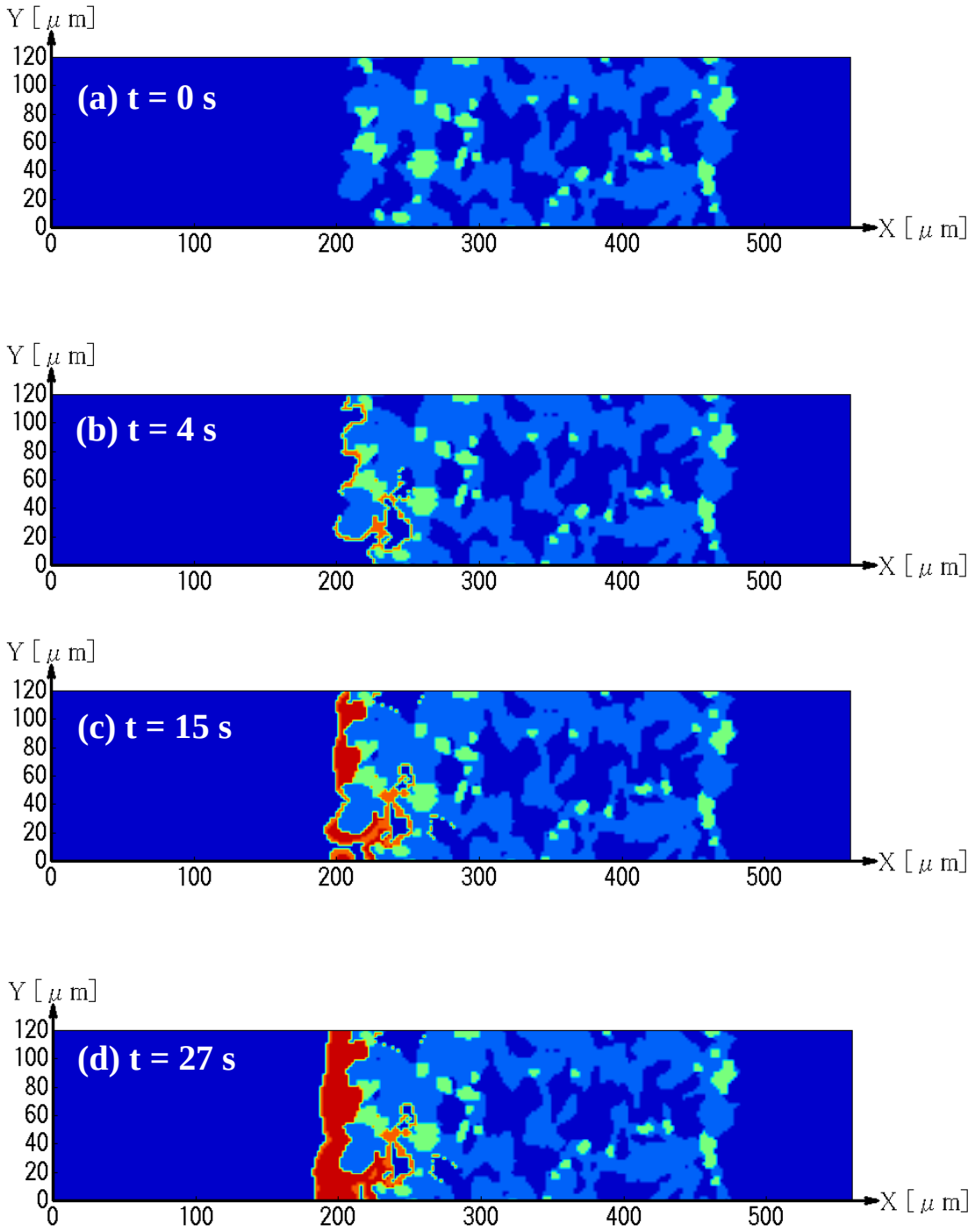

Fig. 7. Profiles of soot deposition region at different times obtained of in-wall CDPF.

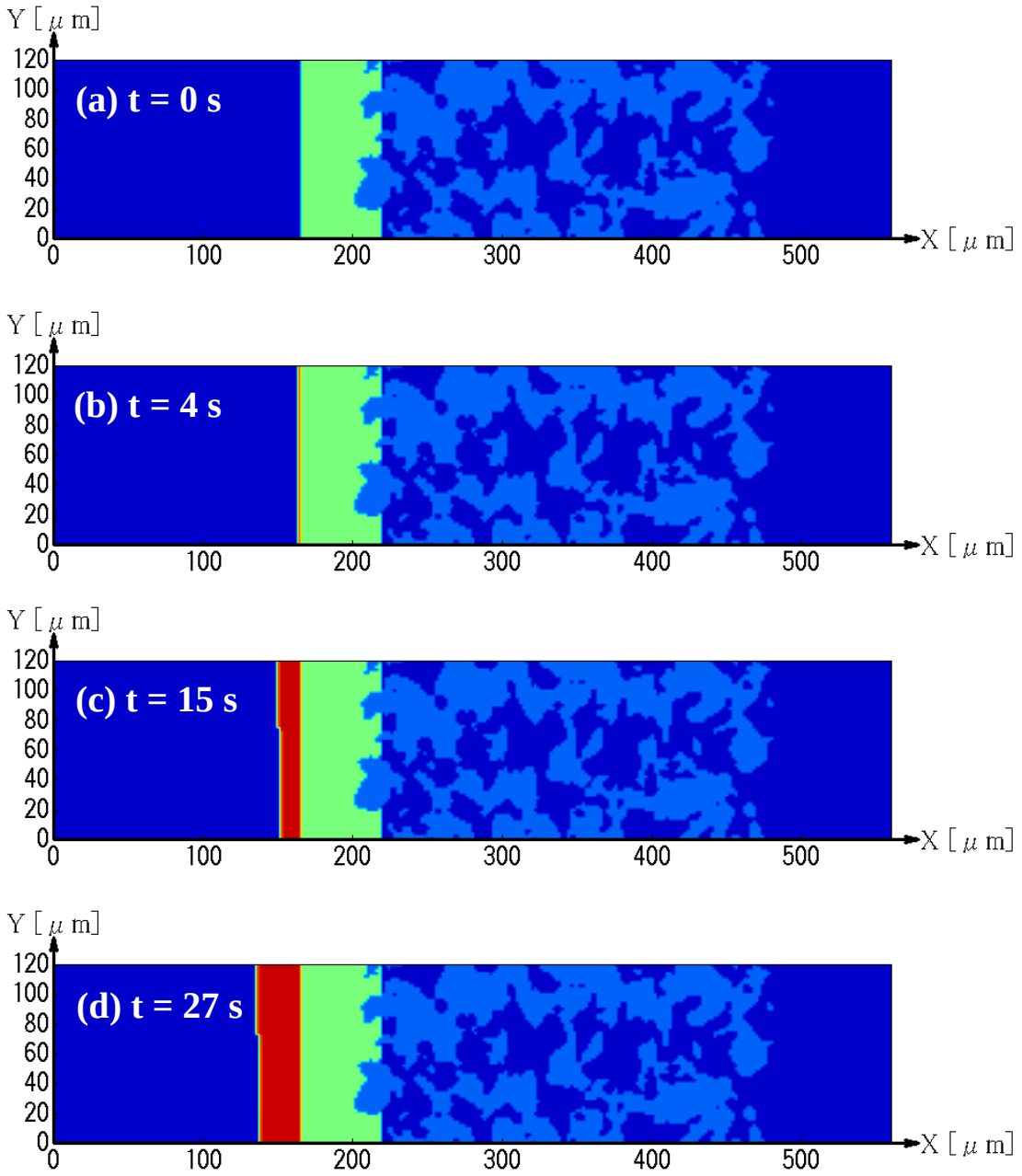

Fig. 8. Profiles of soot deposition region at different times obtained of on-wall CDPF.

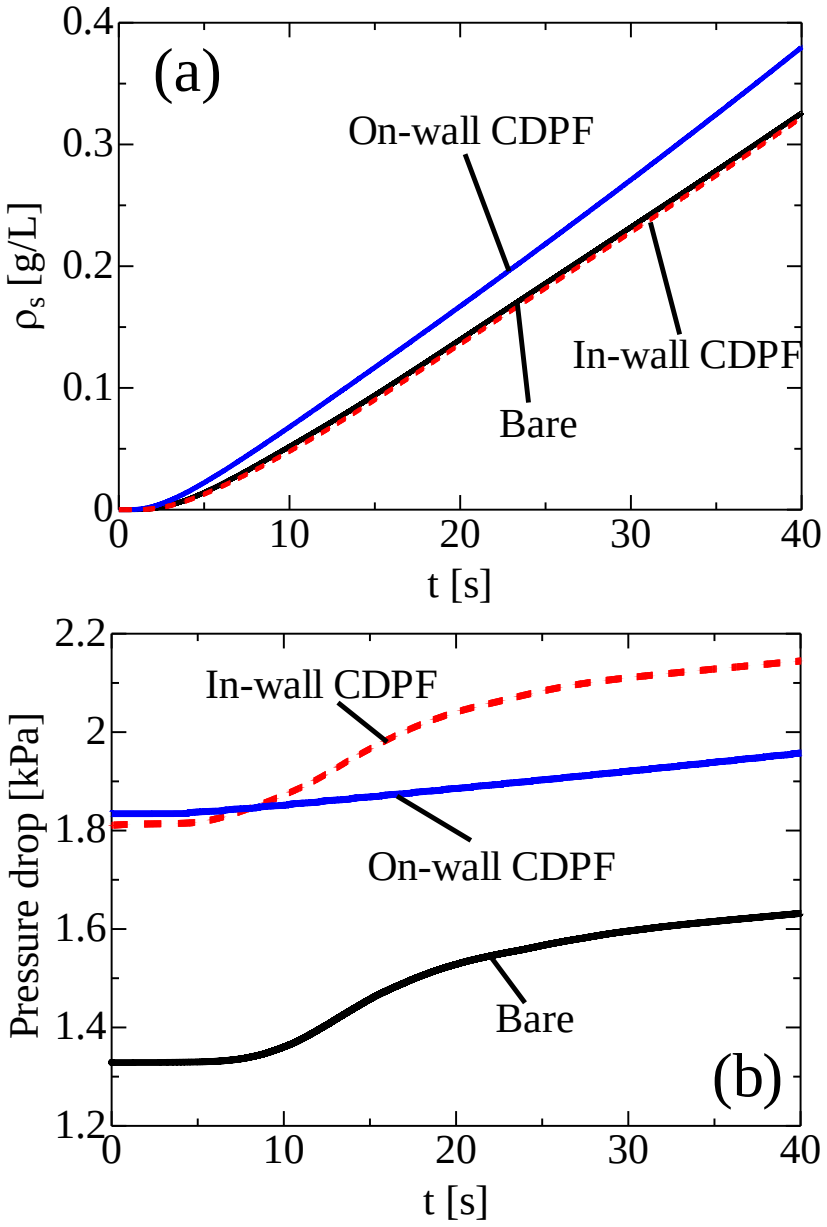

Fig. 9. Time-variations of (a) soot amount and (b) pressure drop

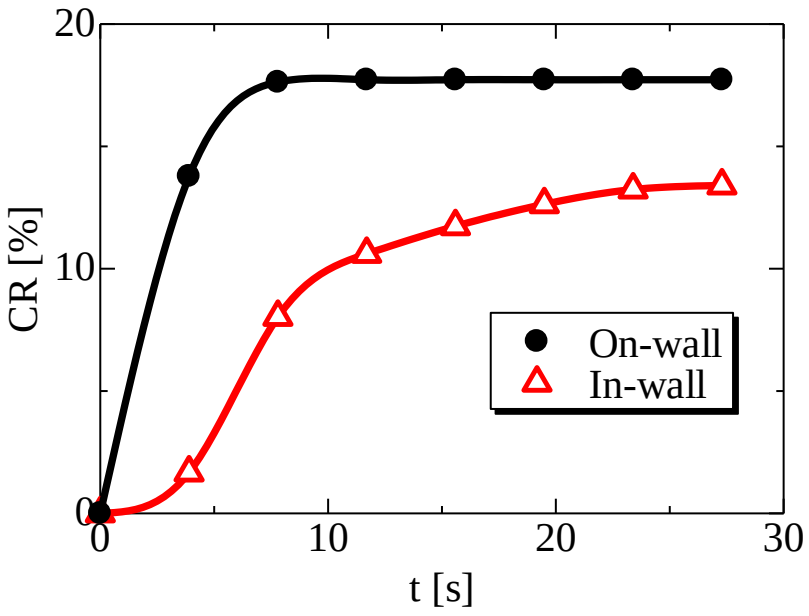

Fig. 10. Time-variation of the contact ratio of in-wall and on-wall CDPFs